Accurate Solution of Periodic Microstrips for Digital Applications

Changhua Wan, *Senior Member, IEEE*, and Jian-X. Zheng, *Member, IEEE*

***Abstract*—This paper presents a conformal-mapping analysis of periodic microstrips (PMSs) with zero-thickness strips. The analysis, for the first time, yields closed-form expressions for the common-mode and alternate-differential-mode capacitances, characteristic impedances, and effective dielectric constants of PMSs. The accuracy of the capacitances against electromagnetic simulations is found to be better than 4% in three test cases. The accuracy of approximating the differential-mode capacitance of PMSs using their alternate-differential-mode one is also found to be within 4%. In the case of an air substrate, the capacitances and impedances become exact. These expressions allow a quick estimate of crosstalk-induced impedance and velocity changes on a signal line at or near the center of a data bus consisting of multiconductor microstrips in digital design. A cell of the periodic structure in an alternate differential mode is actually a single microstrip (SMS) with sidewalls and, therefore, the alternate-differential-mode results are equally useful in the design of such an SMS. As expected, calculated alternate-differential-mode data for a large strip spacing approach corresponding common-mode ones and those of a corresponding SMS without sidewalls.**

***Index Terms*—Data buses, microstrip, multiconductor transmission lines, periodic structures.**

I. Introduction

With the clock frequency already in the gigahertz range, a successful design of modern high-speed digital systems must include a high-frequency (HF) analysis in addition to a digital/low-frequency design. The HF analysis of data buses is a key issue. Such buses are essentially multiconductor transmission lines among which multiconductor microstrips (MMSs) are the most typical. For this reason, this paper focuses on MMSs, while multiconductor coplanar waveguides have been already considered [1].

One method for the analysis of multiconductor transmission lines involves calculating R, L, C, and G matrices [2], [3] and performing SPICE simulation using a SPICE model [4] or transforming the problem to frequency domain, solving it, and transforming the solution back to time domain [5]. SPICE-like time-domain simulation directly using frequency-domain scattering parameters from a full-wave electromagnetic (EM) simulator is a new and different method.[1] These methods are preferably used in final design of a digital system because they tend to be time consuming.

In the integrated circuit (IC) industry, using static L and C matrices or other methods to determine the bounds of the characteristic impedance and propagation delay of a target line in a multiline environment as an equivalent single transmission line is a common practice during an initial design of a digital system [6]. The reason is that this practice is intuitive and simple. The bounds correspond to the common and differential modes that are the two worst cases. Once these bounds are obtained, signal distortion due to reflections with respect to a load impedance and changes in propagation delay can be analyzed for the two cases. Mathematically, for a two-line microstrip structure

$$Z_{c(d)} = \sqrt{\frac{L_{11} \pm L_{12}}{C_{11} \pm C_{12}}} \tag{1}$$

$$D_{c(d)} = \sqrt{\mu_0 \varepsilon_0 \varepsilon_{ec(d)}} = \sqrt{(L_{11} \pm L_{12})(C_{11} \pm C_{12})}. \tag{2}$$

In (1) and (2), $Z_{c(d)}$, $D_{c(d)}$, and $\varepsilon_{ec(d)}$ denote, respectively, common (differential)-mode characteristic impedance, propagation delay, and effective dielectric constant of an equivalent single transmission line, $\pm$ corresponds to the common and differential mode, and $L_{ij}(C_{ij})$ are the elements of the inductance (capacitance) matrix of the structure. In (2), μ_0 and ε_0 are the permeability and permittivity of free space. For this structure, the common and differential modes correspond exactly to the even and odd modes in microwave terminology. For a three-line microstrip structure as an 8-bit bus, formulas similar to (1) and (2) for the center conductor would be

$$Z_{c(d)} \approx \sqrt{\frac{L_{22} \pm L_{21} \pm L_{23}}{C_{22} \pm C_{21} \pm C_{23}}} \tag{3}$$

$$\begin{aligned} D_{c(d)} &= \sqrt{\mu_0 \varepsilon_0 \varepsilon_{ec(d)}} \\ &\approx \sqrt{(L_{22} \pm L_{21} \pm L_{23})(C_{22} \pm C_{21} \pm C_{23})}. \end{aligned} \tag{4}$$

While (1) and (2) are exact, (3) and (4) are approximate. Simulations and measurements have shown that (3) and (4) are adequate only for a structure with a strip spacing/substrate thickness ratio greater than one [6]. For a structure with four or more lines, no similar formulas are available.

For an MMS, a line in the PMS would be a good model for a target line at or near the center of the MMS. The line would experience the heaviest influence of other lines in two extreme cases. The first case corresponds to the common mode where all the signal strips (or nets in digital terminology) are switching in phase, as illustrated in Fig. 1. Also in this figure, strip width and spacing have been denoted as w and s and the substrate thickness and relative dielectric constant have been denoted as h and ε_r for convenience. In this mode, the plane of symmetry between two adjacent strips is a magnetic wall. The other case is called the "alternate differential mode" where adjacent nets are switching out-of-phase, as depicted in Fig. 2. In this case,

Manuscript received June 5, 2002; revised September 24, 2002.
The authors are with Zeland Software Inc., Fremont, CA 94538 USA.
Digital Object Identifier 10.1109/TMTT.2003.808675

[1] *MDSPICE*, Zeland Software, Fremont, CA.

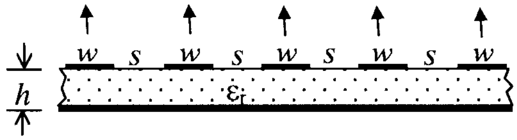

Fig. 1. Cross-sectional view of a PMS in the common mode.

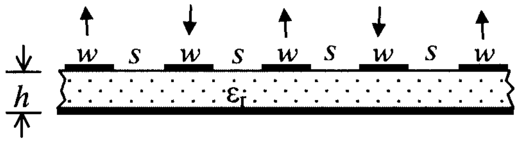

Fig. 2. Cross-sectional view of a PMS in the “alternate differential mode.”

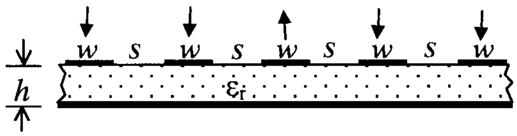

Fig. 3. Cross-sectional view of a PMS in the differential mode.

the plane of symmetry between two adjacent strips is an electric wall. It will be shown that the PMS in the alternate differential mode closely approximates the one in the differential mode where the target line is switching out-of-phase with all the other nets on the bus, as displayed in Fig. 3.

A cell of the PMS in the common mode and alternate differential mode was analyzed in the past, but that analysis involved a “wide” strip assumption in addition to approximate conformal mapping, and the corresponding results are useful only for a structure satisfying the assumption [7]. Two recent analyses [8], [9] both yielded an analytical expression for the capacitance matrix of the PMS, but it is in terms of infinite matrices whose elements require extensive numerical integrations and, thus, is not easy to implement in a computer-aided design (CAD) package. Also, to obtain $Z_{c(d)}$ and $\varepsilon_{ec(d)}$, one has to evaluate the capacitance matrix twice: one for the air substrate and another for the dielectric substrate.

This study aims at developing quasi-static design formulas for quickly calculating the equivalent characteristic impedance and propagation delay of a line in the PMS in the common and alternate differential modes. These formulas will be also useful for a target line at or near the center of the corresponding MMS. Modified conformal mapping will be used to analyze the PMS. A comparison with full-wave simulation data will be presented to demonstrate the accuracy of the formulas.

II. Conformal-Mapping Analysis of PMS

Due to the periodicity in the PMS, a single cell of the periodic structure is taken for conformal-mapping analysis. The following transformation maps the right half of the cell in the z-plane in Fig. 4(a) to the upper half t-plane in Fig. 4(b). Under either the common or alternate differential modes to be discussed shortly, the y-axis coincides with a magnetic wall

$$z = C_1 \int_0^t \frac{(t-k)dt}{\sqrt{t(t-1)(t-m)(t-n)}} + C_2. \tag{5}$$

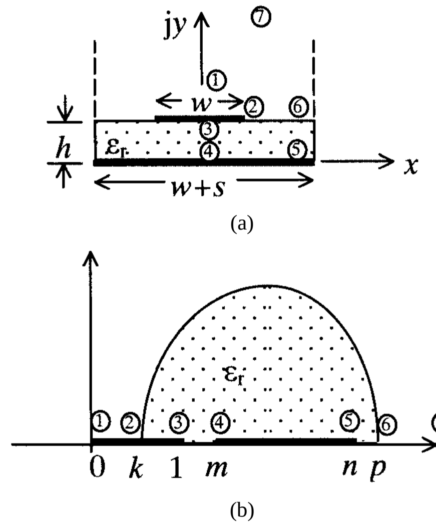

Fig. 4. (a) Cell of a PMS in the z-plane. (b) Mapped half-cell in the t-plane.

The correspondence between important points in the z-plane and those in the t-plane leads to the following equations relating the dimensions in the z-plane to the unknowns in the t-plane

$$\frac{w}{2h} = \frac{n\Pi\left(\alpha, -\frac{1}{n-1}, r\right) + (k-n)F(\alpha, r)}{\Pi\left(\frac{m-1}{m}, r'\right) - kK(r')} \tag{6}$$

$$\frac{w}{2h} = \frac{(1-m)\Pi\left(\gamma, \frac{1}{m}, r\right) + (m-k)F(\gamma, r)}{\Pi\left(\frac{m-1}{m}, r'\right) - kK(r')} \tag{7}$$

$$\frac{w+s}{2h} = \frac{(m-1)\Pi\left(\frac{m-n}{n-1}, r\right) + (1-k)K(r)}{\Pi\left(\frac{m-1}{m}, r'\right) - kK(r')} \tag{8}$$

$$1 = \frac{(n-m)\Pi\left(\beta, \frac{n}{m}, r'\right) + (m-k)F(\beta, r')}{\Pi\left(\frac{m-1}{m}, r'\right) - kK(r')} \tag{9}$$

where

$$r = \sqrt{\frac{n-m}{(n-1)m}} \tag{10}$$

$$r' = \sqrt{1-r^2} \tag{11}$$

$$\alpha = \sin^{-1}\sqrt{\frac{(n-1)k}{n-k}} \tag{12}$$

$$\gamma = \sin^{-1}\sqrt{\frac{m(1-k)}{m-k}} \tag{13}$$

$$\beta = \sin^{-1}\sqrt{\frac{m(p-n)}{n(p-m)}} \tag{14}$$

and $F(\alpha, r)[K(r)]$ and $\Pi(\alpha, \lambda, r)[\Pi(\lambda, r)]$ are incomplete (complete) elliptic integrals of the first and third kinds, respectively.

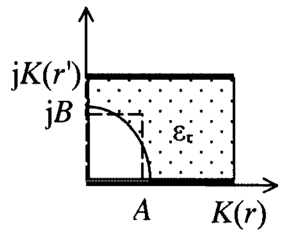

Fig. 5. Equivalent parallel-plate capacitor of the half-cell filled partly by a dielectric and partly by air in the u-plane in the common mode.

A. Common-Mode Case

In the common mode, the plane of symmetry between two adjacent strips is a magnetic wall. The following transformation maps the upper half t-plane in Fig. 4(b) to a rectangle in the u-plane in Fig. 5

$$u = C_3 \int_0^t \frac{dt}{\sqrt{t(t-1)(t-m)(t-n)}}. \tag{15}$$

The correspondence between important points in the t-plane and those in the u-plane gives

$$A = F(\alpha, r) \tag{16}$$
$$B = K(r') - F(\beta, r'). \tag{17}$$

The air–dielectric boundary is close to a quarter of an ellipse and can be approximated by a right-angle bend for capacitance evaluation. Such an approximation has been successfully used in treating both single microstrips (SMSs) [10] and coupled microstrips (CMSs) [11] with approximately 1% accuracy. With an equal-area criterion, the width A' and length B' of an equivalent rectangle would be

$$A' = \frac{\sqrt{\pi}}{2} A \tag{18}$$
$$B' = \frac{\sqrt{\pi}}{2} B. \tag{19}$$

With approximate boundaries either parallel or perpendicular to the electrodes, the total common-mode capacitance of the whole cell is found to be

$$C_c(\varepsilon_r) = 2\varepsilon_0 \varepsilon_r \left[\frac{A'}{K(r') + (\varepsilon_r - 1)B'} + \frac{K(r) - A'}{K(r')} \right] \text{ (F/m)}. \tag{20}$$

Thus, the effective common-mode dielectric constant is

$$\varepsilon_{ec} = \frac{C_c(\varepsilon_r)}{C_c(1)} = \varepsilon_r - \varepsilon_r \frac{A'}{K(r)} \left[1 - \frac{K(r')}{K(r') + (\varepsilon_r - 1)B'} \right] \tag{21}$$

and the common-mode characteristic impedance is

$$Z_c = \frac{\sqrt{\mu_0 \varepsilon_0}}{\sqrt{\varepsilon_{ec}} C_c(1)} = \frac{188.3}{\sqrt{\varepsilon_{ec}}} \frac{K(r')}{K(r)} \ (\Omega). \tag{22}$$

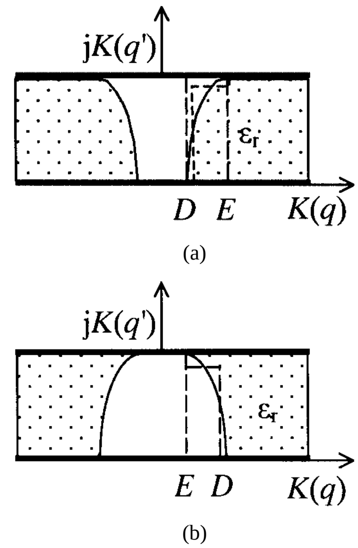

Fig. 6. Equivalent parallel-plate capacitor of the whole cell filled partly by a dielectric and partly by air in the v-plane in an alternate differential mode. (a) $D \le E$. (b) $D > E$.

B. Alternate-Differential-Mode Case

In the alternate differential mode, the plane of symmetry between two adjacent strips becomes an electric wall. Prior to making a further transformation, we mirror the upper half t-plane in Fig. 4(b) so that the whole t-plane represents the whole cell of the periodic structure. The following simple transformation maps the whole t-plane to the upper half u-plane

$$u = \sqrt{t}. \tag{23}$$

The upper half u-plane with symmetric arrangement of the electrodes can then be mapped to a rectangle in the v-plane in Fig. 6 via the Jacobian elliptic function transformation

$$u = \mathrm{sn}(v, q) \tag{24}$$

where

$$q = \frac{1}{\sqrt{m}} \tag{25}$$
$$q' = \sqrt{1 - q^2}. \tag{26}$$

The last transformation results in

$$D = K(q) - F\left(\sin^{-1} \sqrt{\frac{p - m}{p - 1}}, q \right) \tag{27}$$
$$E = F\left(\sin^{-1} \sqrt{k}, q \right). \tag{28}$$

Using the same approximation as used in the common mode, we obtain the total alternate-differential-mode capacitance of the whole cell, as shown in (29), at the bottom of the following page, the effective alternate-differential-mode dielectric constant as shown in the following:

$$\varepsilon_{ead} = \begin{cases} \varepsilon_r - (\varepsilon_r - 1)\dfrac{1}{K(q)} \left[D + \dfrac{\pi(E - D)}{4 + 2\sqrt{\pi}(\varepsilon_r - 1)} \right], \\ \qquad D \le E \\ \varepsilon_r - (\varepsilon_r - 1)\dfrac{1}{K(q)} \left[D - \dfrac{\pi(D - E)}{4\varepsilon_r - 2\sqrt{\pi}(\varepsilon_r - 1)} \right], \\ \qquad D > E. \end{cases} \tag{30}$$

and the alternate-differential-mode characteristic impedance as

$$Z_{ad} = \frac{188.3}{\sqrt{\varepsilon_{ead}}} \frac{K(q')}{K(q)} \; (\Omega). \tag{31}$$

III. Calculation and Validation

Since the formulas derived in Section II are in closed form, calculation is simple. Nevertheless, it is helpful to discuss the calculation in three cases separately.

A. Analysis of PMS With Air or Dielectric Substrate

A key step in analyzing the PMS is to solve (6) [or (7)] and (8) simultaneously for m and n with k found during the process by solving a simple transcendental equation resulting from subtracting (7) from (6). With the range of m and n well defined, i.e., $m > 1$ and $n > m$, Powell's optimization algorithm [12] instead of other methods for nonlinear sets of equations has been used to find m and n. Calculations have shown that, for $0.3 \le w/h \le 4$ and $0.3 \le s/h \le 2.25$, this algorithm produces a solution after an average of six iterations. These ranges are sufficient for digital applications.

In order to validate the proposed technique, calculated capacitances of the PMS in common and alternate differential modes are compared with the data from *IE3D*,[2] a proven method-of-moments-based EM simulator, for corresponding 15-line structures in Table I. Note that the data based on *IE3D* have been obtained using the following calculations with C_{ij} from *IE3D* simulations at 100 MHz:

$$C_c = C_{11} + 2(C_{12} + C_{13} + C_{14} + \cdots + C_{18}) \tag{32}$$

$$C_{ad} = C_{11} - 2(C_{12} - C_{13} + C_{14} - \cdots + C_{18}) \tag{33}$$

$$C_d = C_{11} - 2(C_{12} + C_{13} + C_{14} + \cdots + C_{18}). \tag{34}$$

It is seen that our conformal-mapping-based common-mode and alternate-differential-mode capacitances agree with corresponding *IE3D* simulations to -3.76% and $+2.93\%$. This agreement, therefore, validates the proposed approach. It is also seen that our alternate-differential-mode capacitances agree with *IE3D*'s differential-mode data to -3.94%. This means that approximating the differential-mode capacitance of the PMS using their alternate-differential-mode one is acceptable. The reason is that, in both the differential and alternate differential modes, the first closest line pair relative to the target line dominates the coupling effect than any other pairs, and only the even-order line pairs in the latter are switching out-of-phase with those in the former.

[2]*IE3D*, Zeland Software, Fremont, CA.

TABLE I
CAPACITANCES OF PMS AND 15-LINE MODEL (*IE3D*) WITH DIELECTRIC SUBSTRATE FOR $\epsilon_r = 4.2$

w/h	s/h	C_c/ε_0		$\frac{\Delta C_c}{C_c}$ (%)	C_d/ε_0	C_{ad}/ε_0		$\frac{\Delta C_{ad}}{C_{ad}}$ (%)	$\frac{C_{ad}-C_d}{C_d}$ (%)
		15-line	PMS		15-line	15-line	PMS		
0.5	1.0	4.9699	4.8310	-2.79	8.4388	8.1092	8.1062	-0.04	-3.94
0.5	0.5	3.8967	3.7500	-3.76	10.7130	10.1081	10.4047	+2.93	-2.88
1.0	0.5	5.9936	5.9105	-1.39	13.7995	13.3157	13.3872	+0.54	-2.99

TABLE II
EFFECTIVE PERMITTIVITIES AND CHARACTERISTIC IMPEDANCES OF CMS AND PMS WITH $\epsilon_r = 4.2$ AND THE LAST SUBSCRIPT $e(o)$ MEANING EVEN (ODD) MODE

w/h	s/h	ε_{ee} [14]	ε_{ec}	ε_{eo} [14]	ε_{ead}	Z_e [14]	Z_c	Z_o [14]	Z_{ad}
0.5	1.0	3.1021	3.6252	2.6983	2.6197	112.28	148.47	82.03	75.22
0.5	0.5	3.0966	3.9434	2.6566	2.6030	122.58	199.48	70.52	58.41
1.0	0.5	3.2433	4.0253	2.7174	2.6209	88.48	127.87	54.23	45.55

A comparison of the effective permittivities and characteristic impedances of the PMS in the common and alternate differential modes with those of the CMS in the even and odd modes is made in Table II to see how the PMS differ from the CMS. It is found that the effective permittivity and characteristic impedance of the PMS in the common mode are always larger than those of the CMS in the even mode, while the effective permittivity and characteristic impedance of the PMS in the alternate differential mode are always smaller than those of the CMS in the odd mode.

B. Complete Synthesis of PMS With Air Substrate

When the substrate is air, the capacitance and impedance formulas obtained become exact. Although PMSs with an air substrate will probably never find engineering applications, their exact solution represents a theoretical advance and serves as a benchmark for any other analytical or numerical solutions. Interestingly, synthesis of PMSs is even easier than their analysis. The procedure for the synthesis is discussed in brief below.

For a given Z_{ad}, we can use one of three existing formulas [13] with a relative error of 2.36×10^{-3}, 3×10^{-6}, and 4×10^{-12}, respectively, to find q or q'. Using the formula with a relative error of 2.36×10^{-3}, we obtain

$$q = \frac{e^{\pi/R} - 4}{e^{\pi/R} + 4}, \qquad 0 < R \le 1 \tag{35}$$

or

$$q' = \frac{e^{\pi R} - 4}{e^{\pi R} + 4}, \qquad 1 \le R < \infty \tag{36}$$

where

$$R = \frac{188.3}{Z_{ad}}. \tag{37}$$

$$C_{ad}(\varepsilon_r) = \begin{cases} 2\varepsilon_0\varepsilon_r \left\{ \dfrac{K(q)}{K(q')} - \left(1 - \dfrac{1}{\varepsilon_r}\right) \dfrac{1}{K(q')} \left[D + \dfrac{\pi(E-D)}{4 + 2\sqrt{\pi}(\varepsilon_r - 1)} \right] \right\}, & D \le E \\ 2\varepsilon_0\varepsilon_r \left\{ \dfrac{K(q)}{K(q')} - \left(1 - \dfrac{1}{\varepsilon_r}\right) \dfrac{1}{K(q')} \left[D - \dfrac{\pi(D-E)}{4\varepsilon_r - 2\sqrt{\pi}(\varepsilon_r - 1)} \right] \right\}, & D > E. \end{cases} \quad \text{(F/m)} \tag{29}$$

TABLE III
SYNTHESIS OF PMSs AND SMSs WITH AIR SUBSTRATE

Z_c	Z_{ad}	w/h	s/h
150	50	2.1413	0.3724
140	60	2.0552	0.6444
130	70	1.9480	0.9682
120	80	1.8341	1.3360
110	90	1.7220	1.7482
105	95	1.6681	1.9731
101	99	1.6264	2.1636
Z_s=99.67		1.6264	∞

TABLE IV
PARTIAL SYNTHESIS OF A PMS WITH DIELECTRIC SUBSTRATE WITH $\epsilon_r = 4.2$

m	n	w/h	s/h	ε_{ec}	ε_{ead}	Z_c	Z_{ad}
1.15	1.5	0.7974	1.6096	3.3224	2.7425	93.42	75.35
	2	0.8948	1.8142	3.2138	2.8160	83.13	74.36
	4	0.9769	2.011	3.1100	2.9071	75.76	73.19
SMS[14]		0.9769	∞	ε_{es}=3.0366		Z_s=73.31	
1.4	1.5	0.3413	1.3202	3.3798	2.6260	151.36	94.51
	2	0.4858	1.7289	3.1892	2.7021	112.59	93.17
	4	0.5768	1.9807	3.0497	2.8012	96.55	91.51
SMS[14]		0.5768	∞	ε_{es}=2.9488		Z_s=92.17	
1.49	1.5	0.1894	0.8882	3.5188	2.6024	226.08	99.30
	2	0.4099	1.6935	3.1944	2.6788	122.19	97.88
	4	0.5054	1.9755	3.0409	2.7794	102.06	96.09
SMS[14]		0.5054	∞	ε_{es}=2.9315		Z_s=96.99	

Similarly,

$$r = \frac{e^{\pi/S} - 4}{e^{\pi/S} + 4}, \qquad 0 < S \le 1 \tag{38}$$

or

$$r' = \frac{e^{\pi S} - 4}{e^{\pi S} + 4}, \qquad 1 \le S < \infty \tag{39}$$

where

$$S = \frac{188.3}{Z_c}. \tag{40}$$

Once $r(r')$ and $q(q')$ are available, m and n can be calculated from (25) and (10). k can then be found by solving a transcendental equation, as discussed in Section III-A. Finally, w/h and s/h can be calculated from (6) [or (7)] and (8).

Synthesized w/h and s/h for given Z_c and Z_{ad} are tabulated in Table III together with Z_s, the characteristic impedance of a corresponding SMS for $s/h = \infty$. It is seen that as theoretically expected, Z_{ad} approaches Z_c and Z_s as s/h becomes large.

C. Partial Synthesis of PMSs With Dielectric Substrate

For PMSs with a dielectric substrate, complete synthesis becomes difficult. In contrast, synthesizing w/h and s/h for a given m and n is easy. This synthesis is called partial synthesis here. Sample synthesis data together with those for a corresponding SMS are given in Table IV. It is found that $Z_{ad}(\varepsilon_{ead})$ approaches $Z_c(\varepsilon_{ec})$ as s/h increases and would reach $Z_s(\varepsilon_{es})$ if s/h becomes infinity.

IV. CONCLUSIONS AND DISCUSSIONS

The problem of PMSs under a common mode and alternate differential mode has been treated with modified conformal mapping. This problem closely approximates the two worst cases of a target line at or near the center of MMSs used as data buses. The treatment has led to accurate formulas for the effective dielectric constants, capacitances, and characteristic impedances of a periodic cell of the PMS in these two modes. The capacitances and impedances for structures with an air substrate are exact and can be used as benchmarks. The formulas have been validated by a close agreement between our PMS data and accurate EM simulations. The results presented should be very useful in the design of both high-speed digital buses and microwave couplers.

While its complete synthesis for air–substrate or partial synthesis for dielectric substrate is easy, analysis of PMSs requires solving a nonlinear set of two equations. It is our hope that, in the future, the derived formulas can be simplified or modified eventually to become completely CAD-oriented ones like those for SMSs and CMSs [14].

Effect of strip thickness can be accounted for approximately using either Wheeler's model [15] or its modified version [14].

REFERENCES

[1] G. Ghione, "An efficient, CAD-oriented model for the characteristic parameters of multiconductor buses in high-speed digital GaAs IC's," *Analog Integrated Circuits and Signal Processing*, vol. 5, pp. 67–75, 1994.

[2] C. Wei, R. F. Harrington, J. R. Mautz, and T. K. Sarkar, "Multiconductor transmission lines in multilayered dielectric media," *IEEE Trans. Microwave Theory Tech.*, vol. MTT-32, pp. 439–450, Apr. 1984.

[3] R. F. Harrington and C. Wei, "Losses on multiconductor transmission lines in multilayered dielectric media," *IEEE Trans. Microwave Theory Tech.*, vol. MTT-32, pp. 705–710, July 1984.

[4] V. K. Tripathi and J. B. Rettig, "A SPICE model for multiple coupled microstrips and other transmission lines," *IEEE Trans. Microwave Theory Tech.*, vol. MTT-33, pp. 1513–1518, Dec. 1985.

[5] A. R. Djordjević and T. K. Sarkar, "Analysis of time response of lossy multiconductor transmission line networks," *IEEE Trans. Microwave Theory Tech.*, vol. MTT-35, pp. 898–908, Oct. 1987.

[6] S. H. Hall, G. W. Hall, and J. A. McCall, *High-Speed Digital System Design*. New York: Wiley, 2000.

[7] R. Pregla, "Calculation of the distributed capacitances and phase velocities in coupled microstrip lines," *Arch. Elektr. Ubertragung*, vol. 26, no. 1, pp. 470–474, 1972.

[8] D. Homentcovschi, G. Ghione, C. Naldi, and R. Oprea, "Analytic determination of the capacitance matrix of planar or cylindrical multiconductor lines on multilayered substrates," *IEEE Trans. Microwave Theory Tech.*, vol. 43, pp. 363–372, Feb. 1995.

[9] D. Homentcovschi and R. Oprea, "Analytically determined quasi-static parameters of shielded or open multiconductor microstrip lines," *IEEE Trans. Microwave Theory Tech.*, vol. 46, pp. 18–24, Jan. 1998.

[10] H. A. Wheeler, "Transmission-line properties of parallel strips separated by a dielectric sheet," *IEEE Trans. Microwave Theory Tech.*, vol. MTT-13, pp. 172–185, Mar. 1965.

[11] C. Wan, "Analytically and accurately determined quasi-static parameters of coupled microstrip lines," *IEEE Trans. Microwave Theory Tech.*, vol. 44, pp. 75–80, Jan. 1996.

[12] W. H. Press, B. P. Flannery, S. A. Teukolsky, and W. T. Vetterling, *Numerical Recipes in C*. New York: Cambridge Univ. Press, 1988.

[13] W. Hilberg, "From approximations to exact relations for characteristic impedances," *IEEE Trans. Microwave Theory Tech.*, vol. MTT-17, pp. 259–265, May 1969.

[14] E. Hammerstad and O. Jensen, "Accurate models for microstrip computer-aided design," in *IEEE MTT-S Int. Microwave Symp. Dig.*, Washington, DC, 1980, pp. 407–409.

[15] H. A. Wheeler, "Transmission-line properties of a strip on a dielectric sheet on a plane," *IEEE Trans. Microwave Theory and Tech.*, vol. MTT-25, pp. 631–647, Aug. 1977.

Changhua Wan (M'97–SM'00) received the B.S., M.S., and Ph.D. degrees in electrical engineering from the University of Electronic Science and Technology of China (UESTC), Chengdu, China, in 1983, 1986, and 1991, respectively.

He is currently a Senior Research and Development Engineer with Zeland Software, Fremont, CA, where he develops EM simulation and HF design automation software. He was the principal author of *COCAFIL* (a waveguide filter design suite), *FilterSyn* (a coaxial/planar filter synthesis package), and *LineGauge* (a transmission-line design tool). Prior to joining Zeland Software, he was a Senior Staff Engineer with Quinstar Technology, Torrance, CA, where he was responsible for their antenna products. His other professional experience includes two years of faculty appointment in electrical engineering with the University of Tromsø, Tromsø, Norway, one year of teaching and research in microwave measurement with UESTC, one year of research in microstrip antennas with Villanova University, Villanova, PA, two years of research in monolithic-microwave integrated-circuit (MMIC) characterization with the Katholieke Universiteit Leuven, Leuven, Belgium, and two years of research in computational electromagnetics with the Polytechnic University of Madrid, Madrid, Spain. He has authored or coauthored over 40 journal and conference papers. His areas of research interests include development of new EM simulation and HF design automation software, numerical and analytic techniques in electromagnetics, and microwave measurement theory and techniques.

Dr. Wan was the recipient of the 1991 Second Award for Advances in Science and Technology presented by the Chinese Ministry of Machinery and Electronics.

Jian-X. Zheng (S'89–M'91) received the B.S. and M.S. degrees in electrical engineering from Tsinghua University, Beijing, China, in 1984 and 1986, and the Ph.D. degree in electrical engineering from the University of Colorado at Boulder, in 1990.

He is currently the President of Zeland Software, Fremont, CA, which he founded in 1992. He is the major developer of *IE3D*, a popular method-of-moments-based EM simulator. He is also the major developer of *MDSPICE*, a mixed frequency- and time-domain simulator. Prior to founding Zeland Software, he was a Research and Development Engineer with EEsof (now the Agilent EEsof Division), Westlake Village, CA. His current research interests focus on development of high-performance EM simulation and HF design automation software.